Journal of Materials Research and Technology 33 (2024) 7123–7135

Contents lists available at ScienceDirect

Journal of Materials Research and Technology

journal homepage: www.elsevier.com/locate/jmrt

Effect of the loss on ignition on the unconfined compressive strength of residual clays from Bogotá-Colombia stabilized with cement

Liliana Carolina Hernández García **, Henry A. Colorado Lopera *

CCComposites Laboratory, Universidad de Antioquia UdeA, Calle 70 No. 52-21, Medellín, 050010, Colombia

ARTICLE INFO

Keywords:
Clayey waste
Soil cement
Pavements
Clays
Marginal waste
Soil stabilization
Unconfined compression strength
Plasticity index

ABSTRACT

Organic matter in rock aggregates, such as subgrade, sand, and gravel, originates from the decomposition of organic remains, including plants and domestic waste. The method used to measure the organic matter content in aggregates for infrastructure projects is known as Loss on Ignition (LOI) in which the difference in weight before and after calcination is considered the percentage of loss due to oxides, carbon, nitrogen, phosphorus, and sulfur derived from the organic material. This study compares the compressive strength of three clayey wastes sourced from Bogotá, Colombia, each with different organic matter contents measured by loss on ignition (LOI), mixed with varying cement contents. A total of 153 cylindrical samples were manufactured using a monotonic compression compaction technique with different cement and water dosages. Monotonic compression is a type of test in which a load is applied continuously from zero until failure occurs, without any unloading. The physical characterization was reviewed with plasticity limits, specific gravity (Gs), methylene blue index (M.B.I.), chemical composition with X-ray Fluorescence (XRF) X-ray diffraction (XRD) and SEM micrographs. Through multivariate statistical techniques, compressive strength was correlated with the Water/Cement ratio and the Cement/Residue ratio, resulting in a function that facilitates calculation of cement dosage and water content. The study identified that the response surfaces of clayey residue types exhibit tighter concavity as organic matter content increases, indicating a narrower range for determining optimum moisture content with higher LOI. This experimental investigation aims to explore the feasibility of incorporating clayey waste enhanced with hydraulic cement into materials for infrastructure construction, thereby reducing reliance on natural resources. However, the results indicate that these materials can be utilized in constructing sustainable pavements by applying more rigorous moisture measurement and control techniques to the mixtures. This approach compensates for the use of waste materials by reducing the need for landfills, saving production energy, preventing pollution from material extraction and exploitation, and decreasing gas emissions that contribute to global climate change.

1. Introduction

The excessive exploitation of natural resources is the main cause of the global crisis, and the biggest challenge facing the current generation is the reduction of emissions and carbon footprint on the planet [1]. The 'Bend the Trend 2024' report compares the increase in material consumption over the last 50 years, rising from 8.4 to 13.2 tons per year per inhabitant worldwide. This represents an average growth of 2.3% per year. The construction sector is one of the main sources of environmental degradation, with natural resource consumption estimated at 106.6 billion tons per year and less than 5% of waste being reused [2] such as fly ash, rubber fiber, the reclaimed asphalt pavement (RAP), silica fume, acai ash [3] (see Table 1). There is also abundant research regarding the use of waste materials in soils and construction materials [4–6]. although the composition are very much dependent of the location of the research. Despite efforts to utilize local raw materials in the region [7,8], technical specifications often limit their use in most infrastructure projects [9], although there are large scale successful cases particularly when the use of waste materials is included in the regulation [10,11].

Materials such as compressible clays, organic clays, and peat are strata that typically need to be removed and discarded at construction sites due to their high organic matter content, tendency to swell, absorption capacity, deformability, and low strength [12]. These cohesive

* Corresponding author.
** Corresponding author.
E-mail addresses: carolina.hernandez8@udea.edu.co (L.C. Hernández García), henry.colorado@udea.edu.co (H.A. Colorado Lopera).

https://doi.org/10.1016/j.jmrt.2024.11.081
Received 9 October 2024; Received in revised form 7 November 2024; Accepted 9 November 2024
Available online 10 November 2024
2238-7854/© 2024 Published by Elsevier B.V. This is an open access article under the CC BY-NC-ND license (http://creativecommons.org/licenses/by-nc-nd/4.0/).

materials fall under the category of marginal construction and demolition waste, constituting approximately 11% of all construction and demolition waste [13]. This marginal waste is often utilized in backfilling for landscaping purposes, especially in areas affected by mining activities or road and track conditioning [14].

To enhance the mechanical properties of fillings containing clayey or marginal waste, various mixing technologies involving hydraulic cements, glass, ash, and other manufactured wastes have been studied [15–23]. These physical and chemical modifications aim to reduce absorption, swelling, and the effects of organic materials present in the waste, such as the inhibition of proper hydration in cement-based mixtures, reduced strength, and decomposition caused by biological mechanisms. However, the stabilization of clay wastes with cement requires studying different variables that affect its strength, such as moisture content, material plasticity, and density. These factors must be carefully balanced in the cement content of the mixture during the design process [24,25].

Between 2014 and 2024, nearly 40,000 articles on the mixtures of clay soils with cement have been indexed in major scientific publication databases. The peak in publications occurred in 2023, and this trend is continuing to grow. As illustrated in Fig. 1, Engineering comprises the largest share of publications at 33%, followed by Earth and Planetary Sciences at 19%, and Materials Science at 15%.

Fig. 2 presents the results of unconfined compressive strength (UCS) in kPa from various scientific publications featuring clay materials mixed with hydraulic cement and other strength-enhancing additives. The most utilized dosages range between 7% and 15%, resulting in compressive strengths between 1 MPa and 6 MPa.

To identify the relationship between the cement content, the additive used and the plasticity index of the soil-cement mixtures of the publications in Fig. 2, the cluster analysis was carried out to classify the observations into homogeneous groups with respect to the three variables. The variability of resistance is due to the plasticity of the material, the consistency of the mixture (whether it is fluid or dry), the additive or addition and the cement content. It is observed that in four groups, mixtures with low cement contents, low fluidity and little plasticity register higher strength to unconfined compression, as shown in Fig. 3.

There are several modeling methods for predicting the strength of mixtures between clay materials and hydraulic cement. However, several authors use linear models because of their precision [26,27]. In the literature review, it was identified that the authors focus on measuring the development of long-term resistance (28, 60, and 90 days). However, the building regulations for roads indicate that traffic must be opened 7 days after the mixture is installed [28,29]. For this reason, this research focuses on measuring and predicting strength at that age. Regardless of whether hydraulic cement develops higher long-term strengths, the state at 7 days will define its performance under service load [30].

The American Concrete Institute in its report 230.1R-09 [55], establishes the guidelines for the design, construction, and inspection of soils with cement mixtures, which are ratified by the Portland Cement Association's (PCA) soil stabilization guide [56]. In both documents, soil cement is defined as a compact mixture of soil, Portland or hydraulic cement, and water used for various pavement and foundation applications. It also classifies soil cement into four categories: Cement Modified Soil (CMS), Cement Stabilized Subgrade (CSS), Cement Treated Base

Table 1
Unconfined compressive strength of soils mixed with cement and admixtures.

USCS	AASHTO	Admixture	Liquid limit	Plasticity index	Cement Content	Strength (kPa)	Fuente
CL-ML	A-7	Only Cement	65.9%	25.0%	6.0%	350	[31]
CL	A-7	Nanosilica	43.0%	23.0%	0%	686.5	[32]
SP	A-3	Silica sand	0.0%	0.0%	8.0%	701	[33]
CL	A-6	Nanosilica	36.3%	14.1%	7%	1231	[34]
CL-ML	A-6	Cement II	24.4%	4.2%	9.0%	1300	[35]
GW	A-1-A	Cement bound material	0.0%	0.0%	4.5%	1600	[36]
CL	A-7	Nanosilica	42.4%	15.3%	15%	1800	[37]
CH	A-7	Only Cement	138.0%	95.8%	4%	2000	[38]
GW	A-1-A	RAP_BG2	0.0%	0.0%	5.4%	2700	[36]
CH	A-7	Oil Shale ash	72.0%	42.0%	6.0%	2750	[39]
SP	A-3	Silica_sand2	34.0%	0.0%	6.0%	2900	[40]
SC	A-4	Char	32.0%	9.0%	20%	3800	[41]
CH	A-7	Rubber fiber	137.0%	91.0%	10%	4500	[42]
SC	SC5	Fly ash	15.3%	6.1%	9%	4800	[43]
SC	A-2-6	NRL	21.0%	13.0%	5.0%	5500	[44]
SC	A-4	GGBS_1	27.6%	9.3%	7.50%	5740	[45]
GW	A-1-A	Reclaimed asphalt pavement	0.0%	0.0%	9.0%	5800	[46]
SC	A-4	Only Cement	27.6%	9.3%	12%	5830	[45]
SC	A-6	Nanosilica	30.0%	13.5%	15%	5851.4	[47]
SC	A-2-6	Reclaimed asphalt pavement	23.0%	18.0%	7.0%	6000	[48]
SC	A-4	Silica fume	15.3%	6.1%	9%	6400	[43]
CH	A-7	Fly ash	88.0%	54.0%	25%	6500	[49]
CL	A-7	Graphene oxide	41.5%	19.6%	15.0%	6505	[50]
SC	A-4	Sugarcane bagasse ash	15.3%	6.1%	9%	6510	[43]
CL	A-7	PVA	44.8%	20.2%	15%	7200	[51]
CL	A-6	Titanium slag	33.2%	14.2%	30.0%	8000	[52]
SM	A-7	Acai ash	45.0%	27.0%	9.5%	8200	[43]
SC	A-4	Ground granulated blast-furnace slag	27.6%	9.3%	10%	8316	[45]
SC	A-4	Only Cement	15.3%	6.1%	10%	10500	[43]
SC	A-4	Acai ash	15.3%	6.1%	9%	11000	[43]
CL	A-7	Only Cement	52.8%	25.9%	25%	1300	[53]
SC	A-3	Silty	39.4%	0.0%	25%	1450	[53]
CL	A-7	Only Cement	61.8%	34.3%	17%	1000	[47]
CL	A-7	Only Cement	53.0%	25.0%	22%	683	[48]
CL	A-7	Soil organic	42.0%	25.0%	9%	5000	[12]
CH	A-7	Phosphogypsum	111.9%	67.9%	21.70%	100	[54]
CH	A-7	Phosphogypsum	83.6%	48.6%	16.50%	110	
CL	A-6	Phosphogypsum	38.5%	15.2%	9.50%	460	
ML	A-7	Phosphogypsum	44.0%	12.5%	10.30%	400	

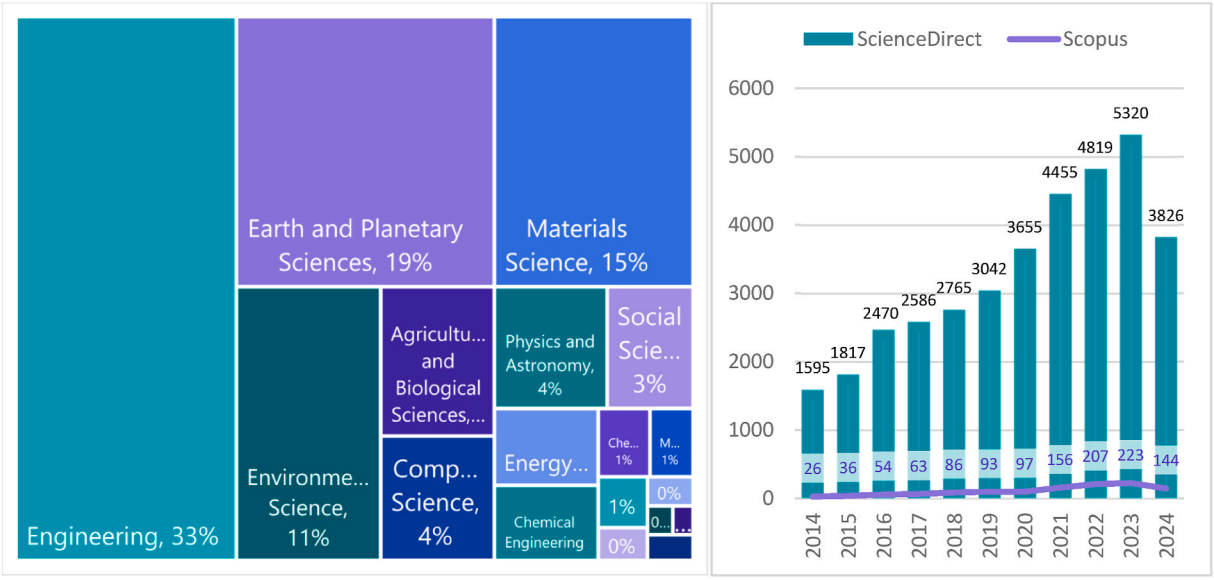


Fig. 1. Papers published in Scopus and Science Direct from 2014 to 2024.

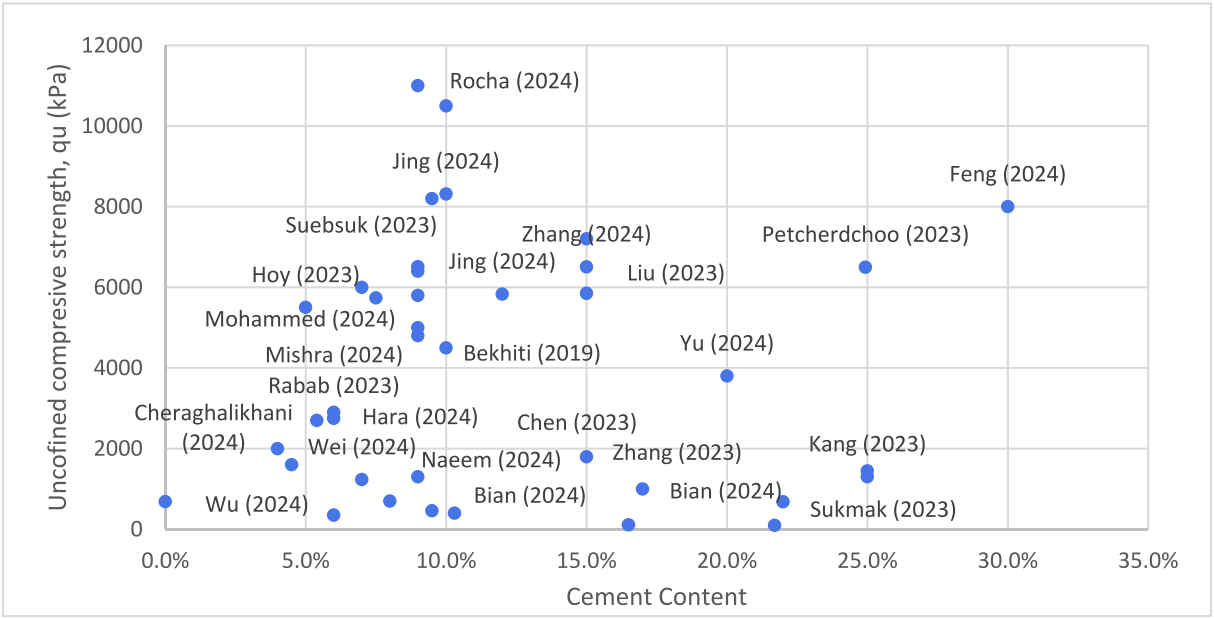


Fig. 2. Unconfined compressive strength from different scientific publications in 2023–2024.

(CTB), and Full Depth Reclamation (FDR).

Cement-modified soil (CMS) is characterized by being composed of fine natural soils of low plasticity, low doses of hydraulic cement, and water. Its function is to improve workability, dehydrate the soil, and increase the speed of construction in rainy areas. This type of treatment enhances the load-bearing capacity of the soil by providing a permanent modification. In this case, the material does not require a maturation period for the application of loads, so the design strength at 7 days is very low, ranging between 690 and 2000 kPa.

On the other hand, Cement Stabilized Subgrade (CSS) is a material with a slightly higher cement content than CMS. Its purpose is to be part of the pavement structure and improve the CBR bearing capacity, shear strength, compressive strength, and shrinkage/swelling deformations after several wetting and drying cycles.

The Cement Treated Base (CTB) is a mixture of manufactured soil that meets a design gradation, a higher cement content than CMS, and water. This material can be prepared on-site or in the plant, and its compressive strength at seven days can range between 2000 and 4000 kPa [57].

FDR (Full Depth Reclamation) is known as the recycled material from deteriorated pavements obtained after the process of milling, crushing, and pulverizing the running surface of the asphalt pavement and the underlying layers, which could be granular or subgrade bases. This scarified material is mixed with cement and water, producing a homogeneous and stabilized compact layer with good structural capacity, as well as the economic and environmental benefits of waste recycling [58].

In that order, the PCA recommends a model for the design of soil-cement mixtures based on soil characterization, compaction percentage, and unconfined compressive strength [59]. On the other hand, the American Association of State Highway and Transportation Officials (AASHTO) defines the design methods for soil-cement mixtures based on

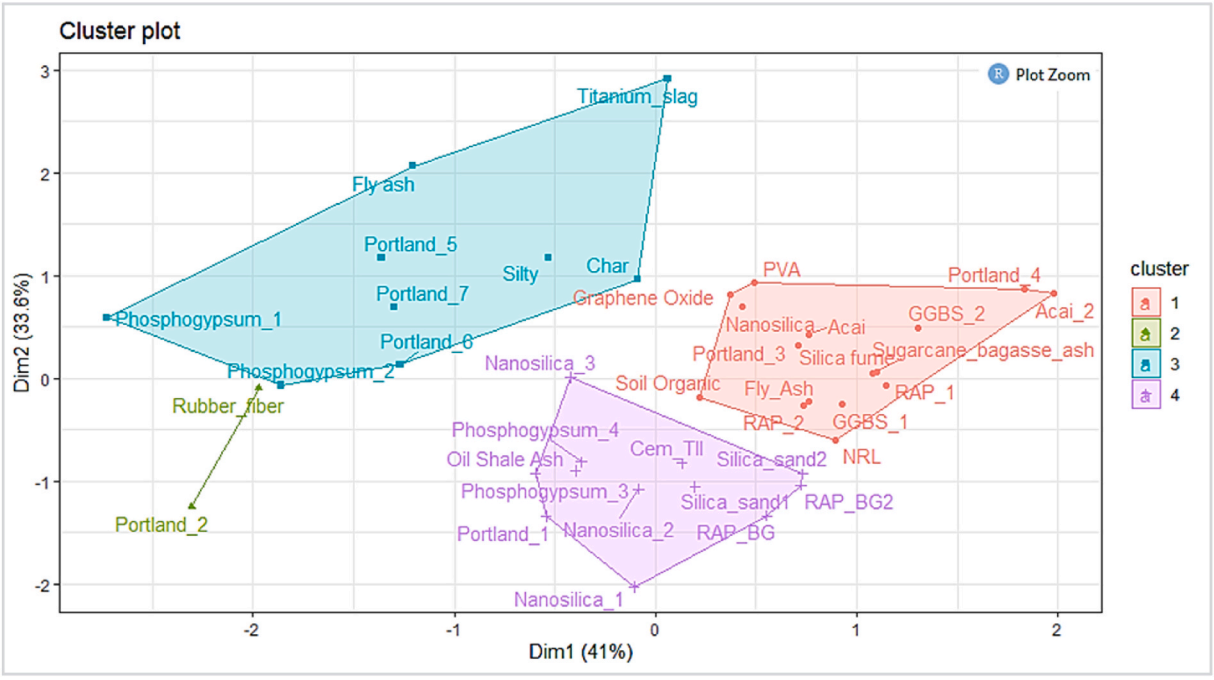


Fig. 3. Non-hierarchical cluster of soil cement with the variables PI, Cement and additive content and unconfined compression.

the moisture-density ratio tests (T134) [60], wetting and drying tests (T135) [61], and freezing and thawing test (T36) [62].

The purpose of the soil cement design is to enhance the mechanical characteristics of the soil in its natural state. However, there are standards that must be met to obtain a cement-stabilized base and subbase. AASHTO, in conjunction with the General Contractors Association (AGC) and the American Road and Transportation Builders Association (ARTBA), developed a Guide Specification for producing Pozzolanic Stabilized Mix (PSM) bases. This guide is now used by the Federal Highway Administration [63], and it is summarized in the following table.

The European standard BS EN 14227–15:2015 has similar standards to those shown in Table 2. It regulates the dosage, construction, and quality control of hydraulically bound soil mixtures for roads, aerodromes, and other traffic areas. This European standard covers soil stabilization using one or a combination of cement, fly ash, hydraulic road binder, lime, and blast furnace slag [78].

Case studies report that road construction using natural soils mixed with cement increases vehicular load capacity, enhances resistance to water softening through chemical bonding of particles, and reduces traffic stresses, thereby providing a stronger platform [79–81]. Additionally, it can reduce the thicknesses required in the pavement structure [57,81]. Incorporating marginal waste into the design and construction of pavements can reduce the excessive exploitation of natural resources, as well as emissions and carbon footprint. For this reason, in this experimental work, the unconfined compressive strength results of clayey waste from excavation and stone aggregate mining, mixed with Portland cement, are modeled to compare the effect of organic matter content on the mix design.

Pavements constructed with cement treated soil are 11% cheaper than those with traditional structures. The results of this research, applied to pavement construction, enhance material performance at a lower cost. The reuse of clay waste reduces the need for transporting granular material, resulting in a solution that can be replicated widely and applied to numerous materials. This method can reduce carbon emissions by approximately 20%, thanks to decreased material transport and a 32% reduction in pavement thickness. Overall, these changes translate to a smaller carbon footprint, shorter construction times, and a more sustainable infrastructure.

2. Materials and methods

The materials used for this modeling were clay wastes sourced from the Colombian capital, as shown in Fig. 4. The first waste is produced from the washing of sedimentary gravels. Its physical classification is fine clayey sand with a maximum nominal size of 0.18 mm and 10% by weight of kaolinite clay, classified as fine non-plastic clayey sand (NP) according to the Unified Classification System (UCS). The second waste is obtained from mining deposits related to the exploitation and washing of sedimentary sands, sourced from the surface of sludge pools. Its mineralogical classification corresponds to kaolinite clay with a plasticity index (PI) of 35. The third waste is used as a filling material from deep excavations in infrastructure projects and corresponds to kaolinite clay with the presence of diatoms, registering a plasticity index (PI) of 60.

The physical and chemical characterization of the three wastes indicates that each has distinct silica, Loss on ignition from 110 °C to 1000 °C, and liquid limit contents that are proportional to each other, as shown in Table 3.

Where LL is the Liquid Limit, PL is the Plastic Limit, PI is the Plasticity Index, Gs is the Specific Gravity, I.A.M. is the Methylene Blue Index (meq/100 g s), LOI is the Loss on ignition from 110 °C to 1000 °C, and NP stands for Not Plastic.

Early high-strength hydraulic cement (ART) was used to manufacture the specimens. Its chemical composition is detailed in Table 4 and compared with the chemical requirements of Portland cement according to ASTM C150/C150M – 22 [74], which corresponds to Portland Cement Type I.

3. Experimental design

During the experiment, 153 cylindrical samples were manufactured and tested for compression after 7 days of curing, following procedure D1633-17 [75]. The samples taken from each waste source were subjected to a drying treatment at 110 °C (230 °F), followed by a crushing process and finally a grinding process, until a homogeneous dust was

Table 2
Test procedures for base and subbase mixtures with cement.

Property	Standard	Test Method	Regulations
Gradation	%Material passing no. 4 > 50%	Sieve analysis of fine and Coarse Aggregates1	ASTM C136/ AASHTO T27 [64]
Abrasion resistance	Sufficient particle resistance to resist degradation and breakage during construction and under repeated traffic loads. Max: 35%	Resistance to degradation of small size coarse aggregate by abrasion and impact on the Los Angeles machine	ASTM C131/ AASHTO T96 [65]
Plasticity	LL<25% PI<4%	Liquid limit, plastic plasticity index of soils	ASTM D4318 [66]
Soundness of aggregates	Sodium Sulfate, Max: 12 Magnesium Sulfate, Max:18	Soundness of aggregates by use of Sodium Sulfate or Magnesium Sulfate	ASTM C88/AASHTO T104 [67]
Harmful components	Sand Content, min.: 15%. Organic matter content, max.: 2%	Equivalent value of soil sand and fine aggregates (indirect measure of the clay content of aggregate mixtures)	ASTM D2419 [68]
Compressive strength	Min: 2500 kPa (7 days) Max: 4500 kPa (7 days)	Manufacture and curing of soil-cement compression and bending test specimens in the laboratory	ASTM D1632 [69] ASTM C593 [70]
Freeze-thaw durability	Mass losses, Max: 14%	Freeze and thaw testing of compacted soil-cement mixtures	ASTM D560 [71]
Maximum dry density and optimal moisture content	According to service load	Moisture-density ratios of soils and soil-aggregate mixtures using a 2.49 kg (5.5 lb) rammer and a 305 mm (12 in.) drop or Moisture-density ratios of soils and soil-aggregate mixtures using a 10 lb. (4.59 kg) rammer and an 18 in (457 mm) drop	ASTM D698 (estándar) [72] o ASTM D1557 (modificado) [73]
Compact density	Min: 95% density maximum	Soil density in place by the sand cone method Density and unit weight of the soil laid using the rubber balloon method	ASTM D1556 [74] ASTM D2167 [75]
Volumetric stability	Swelling, max: 5%	One-dimensional expansion, contraction and pressure increase of soil-lime mixtures	ASTM D3877 [76]
Resilient module	According to service load	Resilient module of unbonded granular base/subbase materials and subgrade soils	AASHTO T274 [77]



Fig. 4. Origin of each of the selected samples a) Waste 1 from washing gravel mining, b) Waste 2 from the sludge pool from the rock sand washing and c) Waste 3 from the filling with material from deep excavations in the city of Bogotá.

obtained that passes through a 200-mesh (75 μm) sieve (see Fig. 5).

Unlike traditional and standardized methods for compacting samples, a specially designed mold was used in this investigation, which complies with the dimensions required by ASTM D1632 [69]. With a diameter of 72 mm and a height of 145 mm, a height/width ratio of 2 is achieved. Compaction was performed using a hydraulic press applying a maximum load of 200 kN. After compaction, the cylinder was removed and stored in a curing booth for 7 days at a temperature of 23 °C and a relative humidity of 98%. Unlike the traditional method, this approach reduces the effect of porosity on the test results [82].

The manufacturing process of the sample involves mixing the specified dosage (by weight) of clay residue, hydraulic cement, and water until a homogeneous mixture with consistent kneading is achieved. Because clay materials tend to form lumps and clods when mixed with water, this effect is mitigated by applying the water using a spray that disperses it evenly. Once the mixture is ready, it is introduced into the mold and tamped with a blunt-point rod of 3/8″ diameter, applying 35 taps in a spiral pattern from bottom to top [76]. The piston is then placed inside the mold, and the sample is compacted using a hydraulic press, starting with the top layer until a load of 200 kN is reached. The collar is removed, the mold is rotated, and then the load is applied again to the underside. Finally, the sample is extracted, its mass is recorded, and it is stored in the curing booth (see Fig. 6).

Three samples of each waste type were produced for each dosage, using four different cement contents and four different water contents. Unconfined compression tests were conducted in accordance with ASTM D4219-11. After seven days of curing, the sample moisture, dry density, and maximum compressive strength were recorded.

The chemical characterization of the materials was performed using X-ray fluorescence (XRF) MLQFRX010. For scanning electron microscopy (SEM) characterization, the samples were fractured, dried for 24 h at 60 °C in an electric oven, and then pulverized to facilitate analysis. The samples were coated with a thin film of gold to enhance conductivity. The equipment used was a JEOL JSM 6700R in a high vacuum mode and its calibration is carried out with the automatic adjustment package.

The tests were conducted using a Malvern Panalytical X-ray diffractometer (XRD) Model Empyrean 2012, equipped with a Pixel 3D detector and a Co source ($\lambda = 1.790307$) at 40 kV and 40 mA. The goniometer was set to Omega/2 theta mode with a platform configuration of Reflection Transmission Spinner, rotating at 4 rpm. The step size was 0.01°, with a time per step of 50 s. A ½° divergence slit and a 1° anti-scattering slit were used. Phase quantification was performed using High Score Plus software with the Rietveld method and the ICSD FIZ

Table 3
Physical and chemical characterization of waste.

Waste	LL	PL	PI	Gs	I.A.M.	Composition (%)						
						SiO_2	Al_2O_3	Fe_2O_3	CaO	MgO	LOI (110-100 °C)	Σ
1	21%	–	NP	2.33	3.40	80.1	8.9	4.4	0.18	2.42	4.0	100
2	59%	24%	35%	2.28	8.20	65.1	16.6	7.92	0.09	3.49	6.8	100
3	90%	24%	66%	1.76	10.00	62.0	16.7	3.7	0.7	3.2	13.7	100

Table 4
Oxide content (%) measured by X-ray fluorescence.

	CaO	SiO_2	$Al2O_3$	SO_3	Fe_2O_3	MgO	P_2O_5	LOI	Σ
Cement	68.04	13.9	4.58	3.06	3.06	3.97	0.137	3.25	100
ASTM C150			6 max.	3.5 max.	6 max.	6 max.		1.1 max	



Fig. 5. Sample Preparation, *(a) natural drying, (b) kiln drying, (c) crushing, (d) abrasive charge for grinding.*

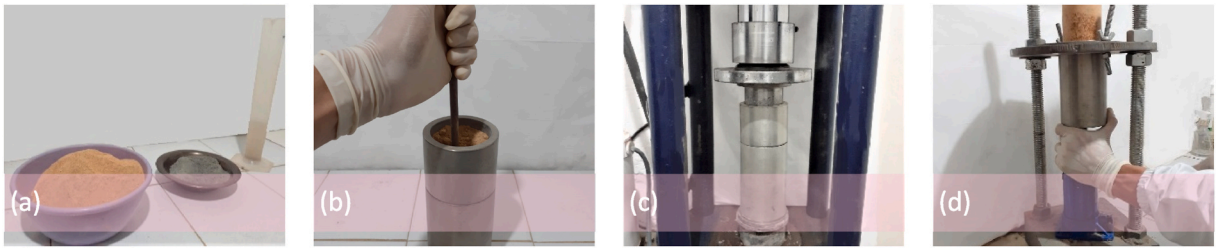


Fig. 6. Processing of cylindrical specimens with a width to height ratio of 1:2.

Karlsruhe 2012-1 database, using rutile as the internal standard.

Data interpretation was carried out through multivariate analysis, employing techniques and models that range from exploratory analysis to the identification of patterns in multivariate data. The variables analyzed included cement content, water-cement ratio, dry density, porosity, void ratio, organic matter content, plasticity index of clay residue, and compressive strength.

For the review of the interrelations between the variables, a significance level of 5% was adopted. The assumptions of normality, independence, multicollinearity, specification, and homoscedasticity were also validated.

4. Results

4.1. Chemical characterization

Using X-ray diffraction (XRD) techniques, the crystalline materials and phase identifications of the wastes used in the mix design were characterized. When compared with previously validated databases, Fig. 7 illustrates the results of the samples, which showed the greatest similarity to the wastes used. The graph highlights the distinctive peaks of quartz (Q), kaolinite (K), and hydraulic cement components such as CSH, calcite ($Ca_6C_6O_{18}$), and lime (Ca_4O_4). Compared to the samples without hydraulic cement, the chemical reaction with kaolin results in the formation of CSH gel, inversely proportional to the organic matter content.

Table 5 shows the composition of the phases of the materials, as defined by the diffraction curves presented in Fig. 7. A trend is observed in the variation of the chemical composition of the mixtures, where part of the kaolinite clay is transformed into calcite and lime. Note how the organic matter content and variations in the chemical composition of the clay contribute to the formation of calcite. Contrary to the findings in the literature review, the residue with the highest organic matter content developed more calcite, while the residue with the lowest organic matter content developed less calcite. It is initially deduced that the organic material retains the water necessary to form calcium bonds in the dry consistency soil-cement mixtures.

Table 6 shows the chemical composition of each mixture. It is observed that the formation of $CaCO_3$ is proportional to the cement content in the mix (see Table 7).

Following the AASHTO T267 and ASTM D999 methodologies, the organic content of the three soils was determined. This method quantifies the oxidation of organic matter by exposing the sample in a furnace for 6 h at 445 °C. The organic content is expressed as a percentage of the mass of the dried soil, as shown in the table.

On the other hand, the SEM micrographs reveal the transformation of the clay mineral (see Fig. 8). Before mixing with hydraulic cement, the structure of the kaolinite clay is observed as slabs. After mixing and at the end of the curing period, these slabs are coated and agglomerated by calcite or calcium carbonate.

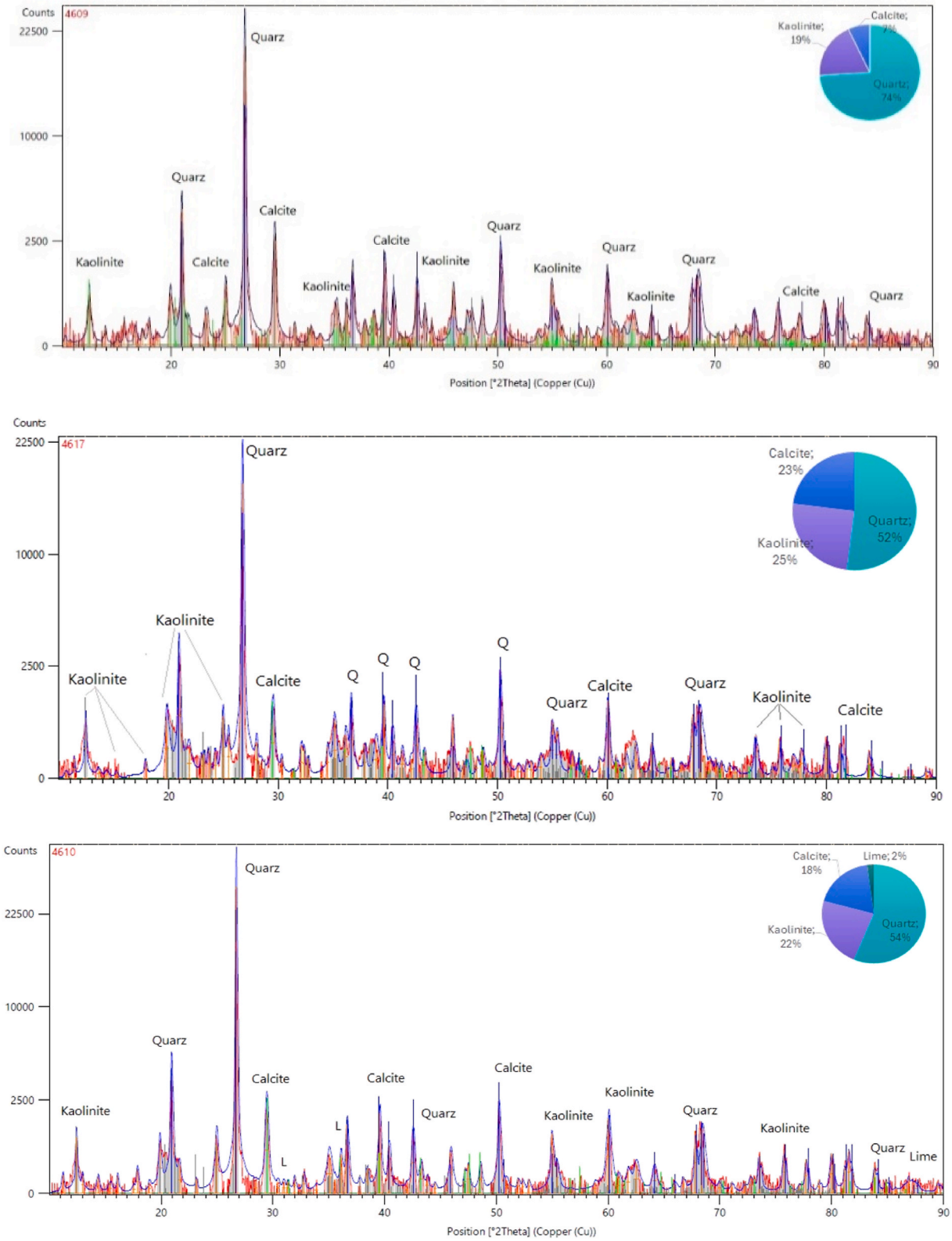


Fig. 7. XRD for mixtures with different clay wastes, waste 1 (4609), waste 2 (4610) and waste 3 (4617).

4.2. Mechanical characterization

A dataset of 153 unconfined compressive strength measurements (in MPa) was collected, using three types of clayey wastes with varying organic matter contents (LOI), different cement contents measured as the ratio of the mass of cement to the mass of the dry sample or soil (C/S), and different water contents measured as the ratio of the mass of water to the mass of the dry sample or soil (W/S).

In the graphical description of the variables shown in Fig. 9, an inversely proportional relationship between LOI and strength is identified. That is, higher organic material content correlates with lower compressive strength. Conversely, higher cement content is associated

Table 5
Semi-quantification by X-ray diffraction - Qualitative.

	Quartz Si_6O_6	Kaolinite $Al_2Si_2O_9H_4$	Calcite $Ca_6C_6O_{18}$	Lime Ca_4O_4
Waste 1	81%	19%		
Waste 1 + Cem	74%	19%	7%	
Waste 2	62%	38%		
Waste 2 + Cem	57%	23%	18%	2%
Waste 3	54%	46%		
Waste 3+Cem	52%	25%	23%	

with increased strength, while a higher water-cement ratio leads to reduced strength. The distribution of the strength data is platykurtic and skewed to the right, indicating that it is not normally distributed. Therefore, an automatic transformation of the variable was applied to validate the model, given by ($UCS_T = UCS^{0.2120646}$), using R Studio.

Where LOI represents loss to ignition by organic material, Strength refers to the unconfined compressive strength in MPa, Cement/Soil denotes the cement content in the mixture by weight, and Water/Cement is the water-cement ratio of the mixture.

To identify any multicollinearity between the variables, the matrix shown in Fig. 10 was reviewed. It reveals correlations between LOI and density, LOI and water content in the mixture, voids and porosity, and density and water content in the mixture. Only untransformed UCS data were used for this plot to validate the multicollinearity of the initial data before developing the model.

On the other hand, there is little to no correlation between cement content and the other variables. Strength (MPa) shows a proportional relationship with cement density and content, while it has an inversely proportional relationship with the void ratio (e), porosity (n), water content in the mixture (W_S), organic matter content (LOI), and water-cement ratio (W_C).

Multicollinearity in a statistical model suggests eliminating variables with factors greater than 0.6 or replacing them with a single variable that represents them. In this case, note that density is collinear with the void ratio and porosity ($n > 0.6$), which, in turn, are collinear with the water content of the mixture ratio (W_S). The latter is related to the water/cement ratio (W_C). To meet the assumption of non-multicollinearity, the water/cement ratio (W_C) is selected as the dependent variable to represent density, water content (W_S), porosity (n), and empty ratio (e). Additionally, the cement content (C_S) is chosen as an intervening variable, while unconfined compressive strength (UCS) is selected as the response variable.

Where LOI represents the loss on ignition by organic material, UCS is the unconfined compressive strength in MPa, Density is the dry density of the sample, e is the void ratio, n is the porosity, W_C is the water/cement ratio, and C_S is the cement content in the mix. To establish the variability between mix design models with different clayey wastes, the response surface was constructed using R Studio, as shown in Fig. 11. This indicates that as the LOI content and plasticity increase, the range of optimum moisture content required to achieve higher compaction and strength becomes narrower.

With 95% reliability, Residue 1, known as clay sand with LOI = 7.45, exhibits a response surface characterized by the model:

Table 7
Mass Loss on ignition by organic matter content, ASTM D999 method.

Waste	Initial mass	Final mass	% Mass Loss on Ignition (LOI)
1	100.0	92.55	7.45
2	100.0	90.48	9.52
3	100.0	83.22	16.78

$$MPa_{SC} = -1.05035 - 23.06507\frac{C}{S} + 19.19359\frac{W}{S} + 74.15867\frac{C}{S}\bullet\frac{W}{S} - 85.56135\frac{C^2}{S} - 95.656\frac{W^2}{S} \quad \text{Eq 1}$$

Where MPa_{SC} represents the strength of sandy wastes, C/S is the mass of cement divided by the mass of dry soil, and W/S is the mass of water divided by the mass of dry soil. With 75% reliability, the response surface is characterized by the following statistically valid model:

$$MPa_{CL} = -1.0732 - 3.7341\frac{C}{S} + 9.4205\frac{W}{S} + 25.1071\frac{C}{S}\bullet\frac{W}{S} - 6.6910\frac{C^2}{S} - 16.2704\frac{W^2}{S} \quad \text{Eq 2}$$

Where MPa_{CL} represents the resistance of clay wastes with medium to low plasticity, C/S is the mass of cement divided by the mass of dry soil, and W/S is the mass of water divided by the mass of dry soil. With 95% reliability, the model for Sample 3, known as high plasticity clay with LOI = 9.52, is given by the following equation:

$$MPa_{CH} = -0.99815 - 5.89264\frac{C}{S} + 5.88862\frac{W}{S} + 10.2887\frac{C}{S}\bullet\frac{W}{S} + 19.07801\frac{C^2}{S} - 6.12125\frac{W^2}{S} \quad \text{Eq 3}$$

Where MPa_{CH} represents the resistance of high plasticity clay wastes, C/S is the mass of cement divided by the mass of dry soil, and W/S is the mass of water divided by the mass of dry soil. To predict the optimal cement content for the mixture, the following model was validated, with a residual error of 0.02147 at 151 degrees of freedom, an R^2 of 0.8185, and an adjusted R^2 of 0.8136. The statistical F-value is 170.2 with 4 and 151 degrees of freedom (Fisher-Snedecor distribution), and the p-value is < 2.2e-16.

$$C = 0.05645 - 1.67756\,LOI^{-1.233872} - 0.15252W^{0.2794664} + 0.25113\,\sigma_{MPa}{}^{0.2120646} \quad \text{Eq 4}$$

Where C is the mass of cement, LOI is loss on ignition, W is the mass of water, and σ_{MPa} is the resistance in MPa. After model validation, the assumptions of normality, homogeneity, constant variance, and residual variability were verified.

After reviewing the assumptions, it is concluded that the model is statistically valid (see Table 8). Fig. 12 shows a graph comparing the laboratory-measured responses with the predicted responses using Equation No. 4. As an example, it is used to calculate the cement content of a mixture required to achieve a strength of 4.5 MPa, with varying LOI values as shown in Table 9:

According to this research, water content depends on the mixing conditions. For dry consistencies, it is recommended to use 3% of the LOI

Table 6
XRF chemical composition of waste mixtures with hydraulic cement.

	$CaCO_3$	SiO_2	MgO	Al_2O_3	Si	K	Ca	Fe	Σ
Waste 1	17.20	45.70	0	3.87	10.74	0.64	18.55	3.29	100
Waste 2	18.49	41.84	0	6.09	18.93	0.80	8.55	5.31	100
Waste 3	21.03	46.4	0.46	5.93	18.41	0.59	5.67	1.53	100

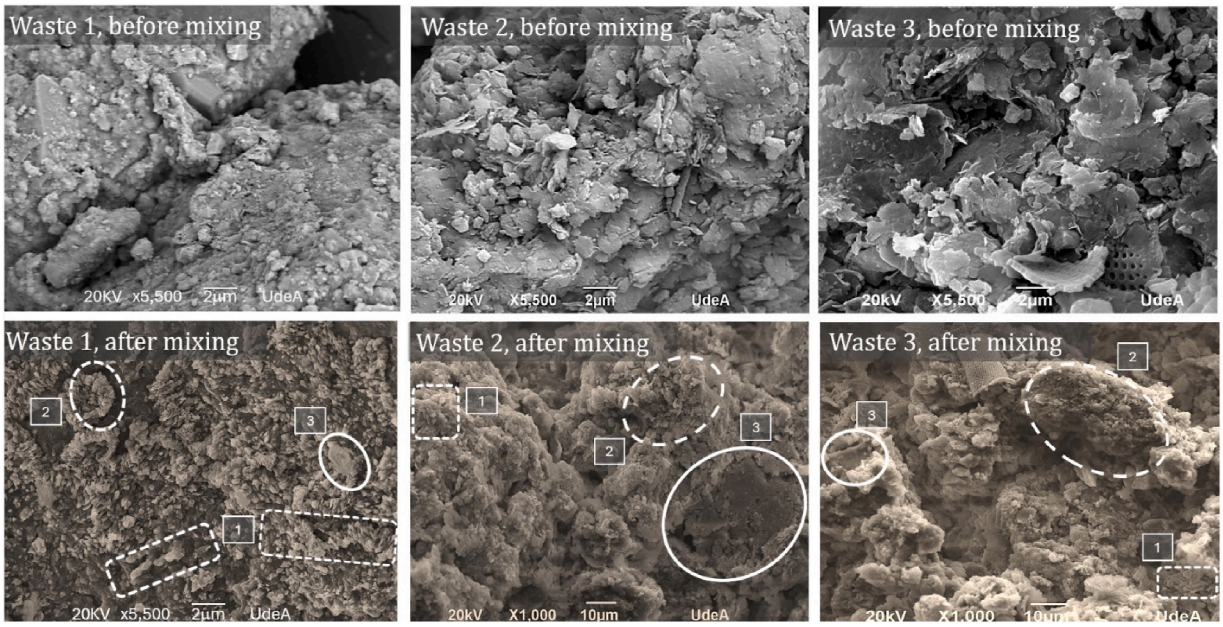


Fig. 8. SEM micrograph of wastes before and seven days after mixing. CSH hydration phases: (1) Portlandite Ca (OH)2, (2) Tobemorite Si2O7H6, and (3) Ettringite.

value. However, given real-world limitations, it is recommended to determine the in-situ moisture content and the moisture reduction once mixed with cement, as this may facilitate calculating the mix moisture factor needed to achieve the results from the equation.

The preparation of the mixtures includes only clay residues, Type I or High Early Strength cement, and water. The results differ from those of mixtures containing additional ingredients such as ash, Nanosilica, recycled asphalt, and others, due to their absorption, granulometry, and chemical composition.

5. Discussion

The clayey wastes used in this research are kaolinite-rich materials with varying proportions and origins, which affect their plasticity and,

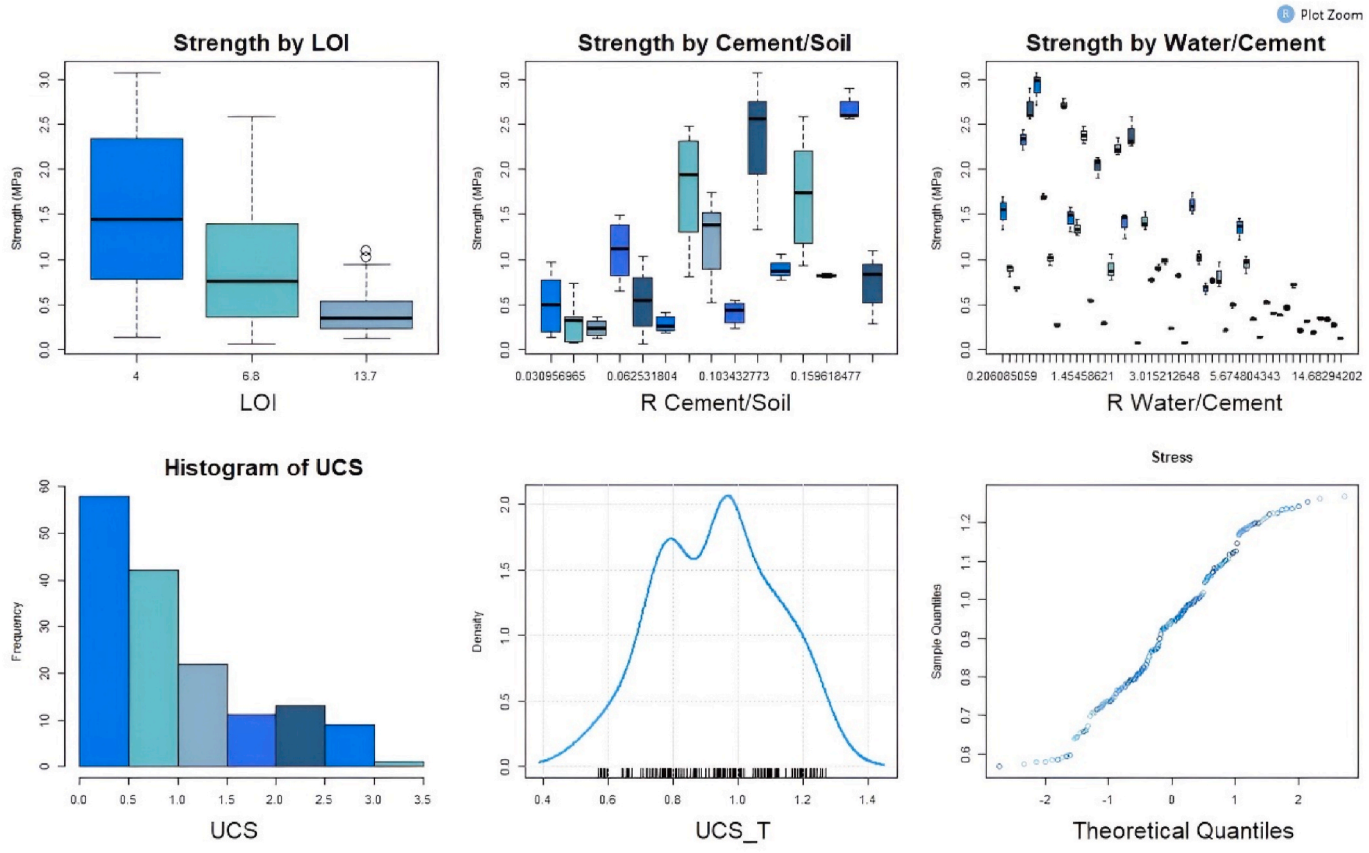


Fig. 9. Graphical description of box and whisker diagrams between the variables of the experiment.

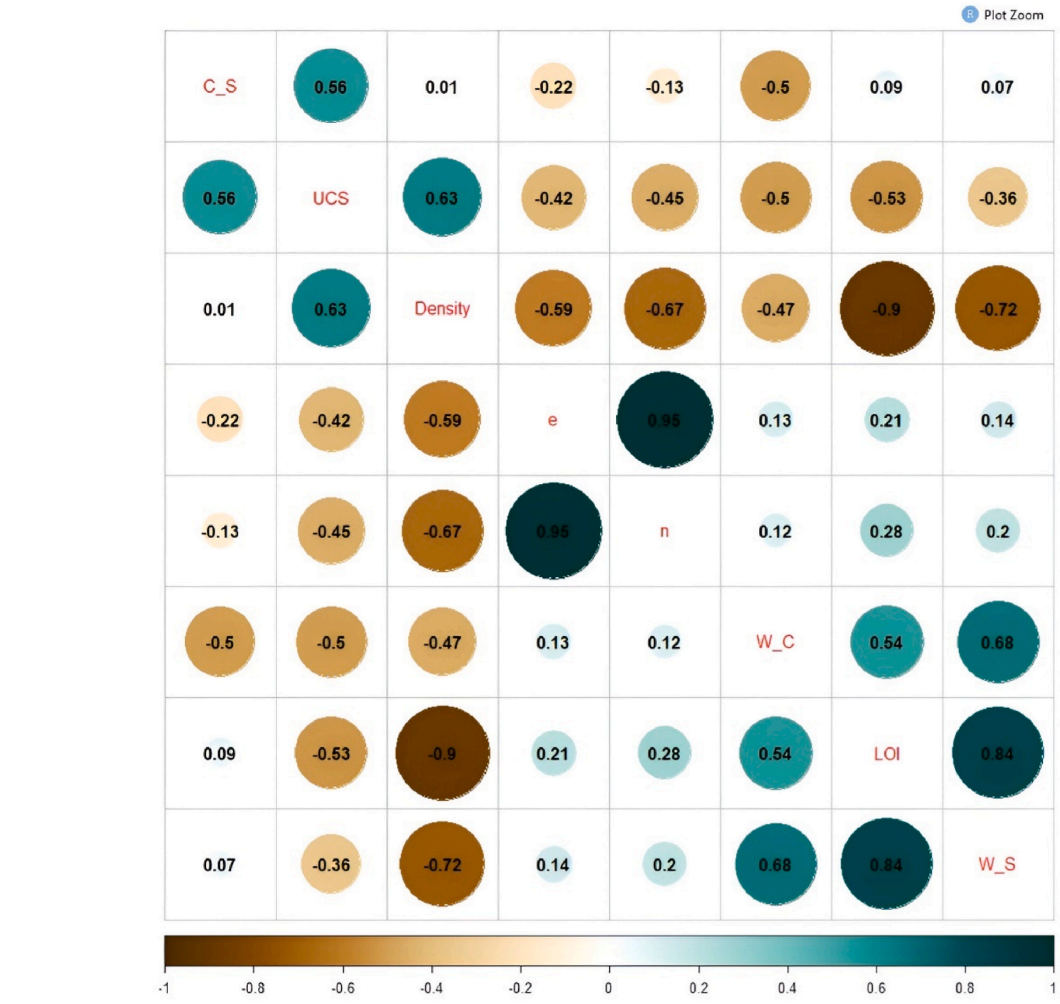


Fig. 10. Multicollinearity matrix between variables.

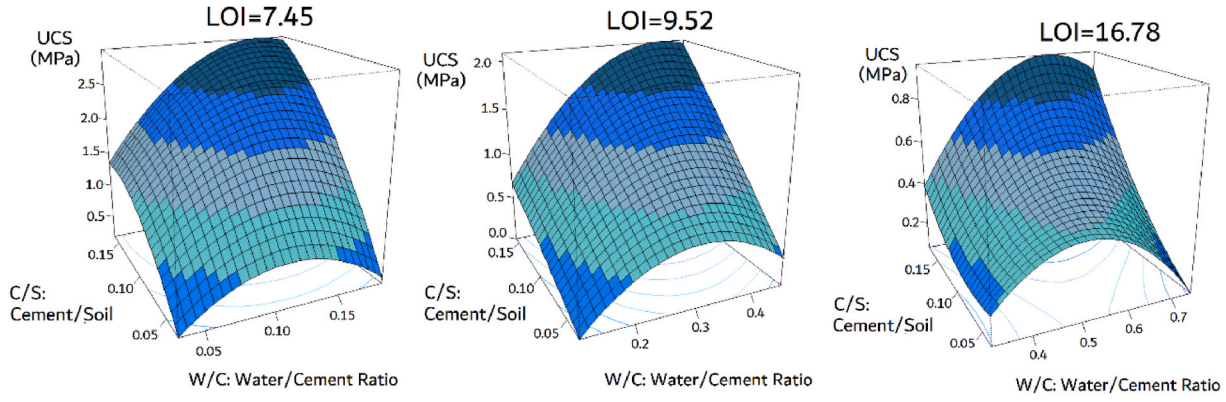


Fig. 11. Response surface of the three samples.

Table 8
Validation of model assumptions made in R Studio.

Supposed	Model	P-value	Validation
Homoscedasticity	Goldfeld-Quandt	0.9995	Not rejected
Normality	Kolmogorov-Smirnov	0.8188	Not rejected
Variance	Anova	2.2e-16	Rejected
Independence	Durbin-Watson	0.35553	Not rejected
Specification	Reset test	0.1316	Not rejected

consequently, their adsorption capacity. Residue 1 is classified as fine sand with a minor proportion of kaolinite clay, while Wastes 2 and 3, due to their plasticity index and liquid limit, are classified as high compressibility clays, and therefore, are considered marginal wastes. All three materials exhibit low activity according to the methylene blue index, indicating low swelling capacity and low chemical instability [83]. This aligns with the characteristics of kaolinite clays.

It is known that the porosity (n) and void ratio (e) of soil-cement mixtures affect the ultimate strength. However, by using the

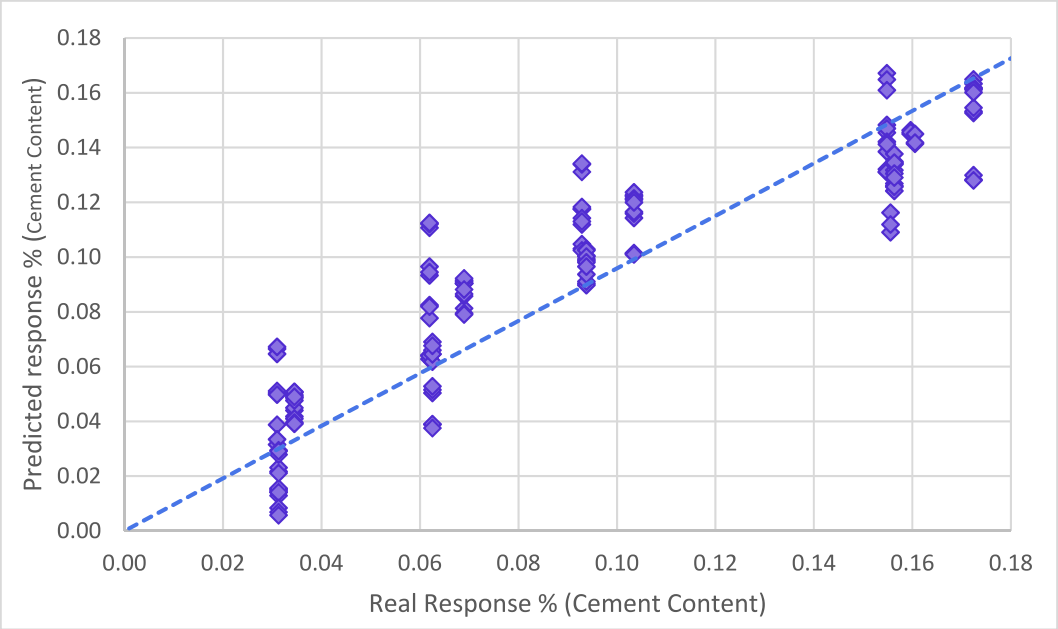


Fig. 12. Graph of actual responses and predicted responses with equation (4) model.

Table 9
Application of equation (4) with different LOI.

LOI	4	6	8	10	12
Water (3%LOI)	12%	18%	24%	30%	36%
σ (Mpa)	4.5	4.5	4.5	4.5	4.5
Cement	1%	12%	17%	20%	21%

monotonic compaction method, it was possible to minimize their impact, resulting in more satisfactory modeling outcomes.

The wastes mixed with Portland cement showed a good development of hydrated calcium as evidenced by X-ray diffraction and SEM micrographs. However, the higher the quartz content, the higher the unconfined compressive strength. This indicates that the LOI content directly affects the mix design and in turn the water content.

A waste with higher organic matter content requires a higher cement content in the mix to achieve higher strength. The response surfaces showed that compressive strength was higher with the lowest LOI content (7.45), while the waste with the highest LOI content (16.78%) achieved only a third of the strength of the sample with the lowest LOI. This confirms that the higher the LOI content, the lower the unconfined compressive strength.

The concavity of the response surfaces indicates that the optimum moisture range becomes narrower as the LOI increases. It is well known that the disposal and final management of marginal soils with high compressibility and high organic matter content generate additional costs in pavement construction. It is important to note that their reuse implies higher costs in cement stabilization and requires stricter moisture control. In regions with fluctuating moisture conditions, specialized machinery and equipment must be available on site to achieve a homogeneous mixture and ensure greater precision in adding the optimal moisture to the mix. Once installed and compacted, it is recommended to work in short sections and cover it with the next pavement layer as soon as possible to avoid alterations in curing due to moisture variability in the area or climate conditions.

6. Conclusions

The graphical exploration of the results reveals significant variance in strength as a function of the LOI content of the material. Additionally, the compressive strength results range from lower to higher values depending on the cement content. Given the involvement of three wastes with different compositions and physical characteristics, the dispersion of results is more pronounced. However, through statistical transformations, it is feasible to construct a model that accurately captures the variances among the three materials.

When comparing the results obtained in this research with those from other publications (Table 1), similar trends can be observed. However, the characterization of materials and cement differs. Soils improved with gravel and sand exhibit higher strength compared to waste that is solely clayey. The type of cement, lime content, and the compaction method used for the sample are also factors that influence the result.

The key variables in the mathematical model are the water content in the mix, the LOI content of the material, the cement content, and the density of the mix. During the manufacturing stage, special care must be taken with the application of the optimum moisture content. The response surfaces for the three materials revealed a more pronounced concavity for those with high plasticity and high LOI content. If the water dosage is altered during the manufacturing or construction stage—due to excess soil moisture, rain, or dehydration from high temperatures—resistance should be compensated by increasing the cement content.

This may explain why laboratory-designed mixtures often show variations in resistance when measured on-site. For sandy materials, variations in water content in the mix do not significantly affect strength. However, for cohesive materials with high plasticity and high LOI content, strength is achieved only within a narrow range of optimum water content. A mixture with high moisture content tends to be cohesive and viscous, while a mixture with low water content can become overly dry. In both cases, strength deteriorates more rapidly compared to sandy or low plasticity materials.

Moisture variation in the mix can be compensated for by increasing the cement content, ensuring that the design strength is achieved during the construction process. Both moisture content and cement content are described in Equations (1)–(3), which characterize the behavior of the response surfaces for the three materials.

To consolidate the three intervening variables in the response variable, a linear correlation model was validated to calculate the cement content required to achieve the design strength in pavement structures,

subgrade, or foundation soils. This allows for the use of waste with characteristics similar to those of the materials used in this study in the construction of infrastructure projects.

According to the results, during the construction stage of a soil cement composed of clayey residues with high organic matter content, the moisture of the mixture, its homogeneity, and, as observed in the SEM micrographs, the curing time must be controlled more rigorously to enhance the development of CSH bonds. One alternative is to cover the layer with another material from the pavement structure as quickly as possible. The moisture retained by the organic material is absorbed by the hydraulic cement, transforming it into calcite and mitigating the effects of expansiveness and swelling.

CRediT authorship contribution statement

Liliana Carolina Hernández García: Conceptualization, Methodology, Investigation, Writing – review & editing. **Henry A. Colorado Lopera:** Conceptualization, Methodology, Investigation, Supervision, Funding acquisition.

Data availability

Data will be fully available upon request.

Funding

This research did not receive Funding.

Declaration of competing interest

The authors declare that they have no known competing financial interests or personal relationships that could have appeared to influence the work reported in this paper.

Acknowledgements

Authors want to acknowledge to Universidad de Antioquia for the doctoral fellowship to Liliana Carolina Hernández García.

References

[1] Creutzig Feliz, et al. 8 transport: climate change. Mitigation of climate change. 2014. New York.
[2] Guerra BC, Leite F, Faust KM. 4D-BIM to enhance construction waste reuse and recycle planning: case studies on concrete and drywall waste streams. Waste Management Oct. 2020;116:79–90. https://doi.org/10.1016/j.wasman.2020.07.035.
[3] Hernández García LC, Monteiro SN, Lopera HAC. Recycling clay waste from excavation, demolition, and construction: trends and challenges. Multidisciplinary Digital Publishing Institute (MDPI); Jul. 01, 2024. https://doi.org/10.3390/su16146265.
[4] Fakhrabadi A, Choobbasti AJ, Kutanaei SS. Durability Evaluation of clayey sandy soil stabilized with eopper-slag-based ceopolymer under freezing–thawing cycles. International Journal of Pavement Research and Technology 2023. https://doi.org/10.1007/s42947-023-00341-8.
[5] Kutanaei SS, Afrakoti MTP, Choobbasti AJ. Effect of coal waste on grain failure of cement-stabilized sand due to compaction. Arabian J Geosci Jun. 2021;14(12). https://doi.org/10.1007/s12517-021-07392-w.
[6] Ghadakpour M, Choobbasti AJ, Kutanaei SS. Experimental study of impact of cement treatment on the shear behavior of loess and clay. Arabian J Geosci Feb. 2020;13(4). https://doi.org/10.1007/s12517-020-5181-7.
[7] García EF, Pérez AC, Colorado HA. Kaolinite-based clay ceramics blended with residual fique fibers for potential plastic soil applications. Int J Appl Ceram Technol Jul. 2021;18(4):1086–96. https://doi.org/10.1111/ijac.13754.
[8] Jiménez JE, Fontes Vieira CM, Colorado HA. Composite soil made of rubber fibers from waste Tires, blended sugar tane colasses, and kaolin clay. Sustainability Feb. 2022;14(4). https://doi.org/10.3390/su14042239.
[9] A. A. of S. H., Aashto TO. Mechanistic Empirical pavement design guide. Washington: AASHTO; MEPDG-3, 2020.
[10] Agudelo G, Palacio CA, Neves Monteiro S, Colorado HA. Foundry sand waste and residual aggregate Evaluated as eozzolans for concrete. Sustainability Aug. 2022;14(15). https://doi.org/10.3390/su14159055.
[11] Agudelo G, Cifuentes S, Colorado HA. Ground tire rubber and bitumen with wax and its application in a real highway. J Clean Prod Aug. 2019;228:1048–61. https://doi.org/10.1016/j.jclepro.2019.04.353.
[12] Hashim Mohammed S, Saeed KA, Ibrahim Al Shaikhli H. Evaluation of the strength and microstructural characteristics of stabilized organic clay soil. Case Studies in Chemical and Environmental Engineering 2024;9(Jun). https://doi.org/10.1016/j.cscee.2024.100647.
[13] PIARC. Review of Practices using marginal and secondary materials in pural and rndustrial areas. Comité Técnico AIPCR Geotecnia y carreteras sin pavimentar. 2019.
[14] Janani R, Kaveri V. A critical literature review on reuse and recycling of construction waste in construction industry. In: Materials Today: troceedings. Elsevier Ltd; 2020. p. 3077–81. https://doi.org/10.1016/j.matpr.2020.09.015.
[15] Ahmadi M, et al. Effects of melt-state shear homogenization on catalytic pyrolysis of mixed plastic waste for feedstock recycling. Materials Today Sustainability 2023;22(Jun). https://doi.org/10.1016/j.mtsust.2023.100343.
[16] Cobo-Ceacero CJ, et al. Effect of the addition of organic wastes (cork powder, nut shell, coffee grounds and paper sludge) in clays to obtain expanded lightweight aggregates. Bol Soc Espanola Ceram Vidr Jan. 2023;62(1):88–105. https://doi.org/10.1016/j.bsecv.2022.02.007.
[17] Nguyen MD, et al. Investigation on the suitability of aluminium-based water treatment sludge as a sustainable soil replacement for road construction. Transportation Engineering 2023;12(Jun). https://doi.org/10.1016/j.treng.2023.100175.
[18] Xavier GTM, Urzedo AL, Nunes RS, Fadini PS, Carvalho WA. Incorporation of clay-based adsorbent into polyvinylidene fluoride membrane for enhanced phosphorus capture in aqueous solution. Resour Conserv Recycl 2023;190(Mar). https://doi.org/10.1016/j.resconrec.2023.106867.
[19] Bòto ML, Dias SM, Crespo RD, Mucha AP, Almeida CMR. Removing chemical and biological pollutants from swine wastewater through constructed wetlands aiming reclaimed water reuse. J Environ Manage 2023;326(Jan). https://doi.org/10.1016/j.jenvman.2022.116642.
[20] Dubale M, Vasić MV, Goel G, Kalamdhad A, Singh LB. Utilization of construction and demolition mix waste in the fired brick production: the impact on mechanical properties. Materials Jan. 2023;16(1). https://doi.org/10.3390/ma16010262.
[21] Dang HTT, Pham LTN, Pham TT, Nguyen HX, Tran NTH, Nguyen KM. Effect of biowaste and construction waste additives on mechanical dewaterability of lake sediment for brick production. J Air Waste Manage Assoc 2023;73(8):625–37. https://doi.org/10.1080/10962247.2023.2228265.
[22] Belioka MP, Markozanne G, Chrissopoulou K, Achilias DS. Advanced plastic waste recycling—the effect of clay on the Morphological and mhermal behavior of recycled PET/PLA sustainable blends. Polymers Jul. 2023;15(14). https://doi.org/10.3390/polym15143145.
[23] Obeng E, Essandoh HMK, Akodwaa-Boadi K, Taylor TS, Kusi I, Appiah-Effah E. Recycled clay bricks and palm kernel shell as constructed wetland substrate for wastewater treatment: an engineered closed circuit circular economy approach. Environ Technol Innov 2023;32(Nov). https://doi.org/10.1016/j.eti.2023.103324.
[24] Mishra A, Dixit A, Singh AK, Das SK. Strength, deformation, and environmental impact assessment of cement stabilized mine overburden soil. J Clean Prod Apr. 2024;447. https://doi.org/10.1016/j.jclepro.2024.141475.
[25] Sukmak G, Sukmak P, Horpibulsuk S, Arulrajah A, Horpibulsuk J. Generalized strength prediction equation for cement stabilized clayey soils. Appl Clay Sci 2023;231(Jan). https://doi.org/10.1016/j.clay.2022.106761.
[26] Kang Go, sang Kim Y, goo Kang J. Predictive strength model of cement-treated fine-grained soils using key parameters: tonsideration of the total water/cement and soil/cement ratios. Case Stud Constr Mater 2023;18(Jul). https://doi.org/10.1016/j.cscm.2023.e02069.
[27] Zhang C, et al. Efficient machine learning method for evaluating compressive strength of cement stabilized soft soil. Constr Build Mater 2023;392(Aug). https://doi.org/10.1016/j.conbuildmat.2023.131887.
[28] ACI. Report on soil cement (ACI 230.1R-09). American Concrete Institute; 2009.
[29] Portland Cement Association, 'Cement-stabilized subgrade (CSS) soils and cement modified soils (CMS) case Histories', PCA American Cement Manufactures.
[30] Conner JR. Guide to improving the effectiveness of cement-based stabilization/solidification. Portland Cement Association; 1997.
[31] Wu Y, Liu X, Yang J, Liu Q. Influence of the wide range cement content on the properties of cement–treated marine soft soil and bound method of semi–solidified soil. Case Stud Constr Mater 2024;20(Jul). https://doi.org/10.1016/j.cscm.2024.e03180.
[32] Cheraghalikhani M, Niroumand H, Balachowski L. Micro- and nano-Illite to improve strength of untreated-soil as a nano soil-improvement (NSI) technique. Sci Rep Dec. 2024;14(1). https://doi.org/10.1038/s41598-024-61812-x.
[33] Naeem M, Arab MG, Elbaz Y, Omar M, Ezzat H, Zeiada W. Resilient behavior of bio-cemented sandy soil treated with enzyme-induced carbonate precipitation for pavement applications. Constr Build Mater 2024;411(Jan). https://doi.org/10.1016/j.conbuildmat.2023.134434.
[34] Wei W, Erlu W, Shuaishuai H, Xingjiang S, Na L, Ping J. Experimental investigation on static and dynamic properties of nanosilica modified cement soil. Constr Build Mater 2024;412(Jan). https://doi.org/10.1016/j.conbuildmat.2023.134746.
[35] Nazari Z, Tabarsa A, Latifi N. Effect of compaction delay on the strength and consolidation properties of cement-stabilized subgrade soil. Transportation Geotechnics 2021;27(Mar). https://doi.org/10.1016/j.trgeo.2020.100495.
[36] Andryanti DM, Phan TM, Lee DW, Park DW. Impact of cement content in cement bound materials on the reflection cracking performance of asphalt pavements. Case Stud Constr Mater Jul. 2024;20. https://doi.org/10.1016/j.cscm.2024.e03229.

[37] Chen Q, Rong H, Tao G, Nimbalkar S, Xie K. Fatigue characteristics of nano-SiO2 cemented soil under coupled effects of dry-wet cycle and seawater corrosion. Constr Build Mater 2023;401(Oct). https://doi.org/10.1016/j.conbuildmat.2023.132579.
[38] Hara H, Ikeda K, Yoshimoto N. Strength reduction mechanism of cement-treated soil under seawater environment. Soils Found Feb. 2024;64(1). https://doi.org/10.1016/j.sandf.2024.101425.
[39] Rabab'ah SR, Sharo AA, Alqudah MM, Ashteyat AM, Saleh HO. Effect of using Oil Shale Ash on geotechnical properties of cement-stabilized expansive soil for pavement applications. Case Stud Constr Mater Dec. 2023;19. https://doi.org/10.1016/j.cscm.2023.e02508.
[40] Mishra A, Dixit A, Singh AK, Das SK. Strength, deformation, and environmental impact assessment of cement stabilized mine overburden soil. J Clean Prod Apr. 2024;447. https://doi.org/10.1016/j.jclepro.2024.141475.
[41] Yu H, Joshi P, Lau C, Ng K. Novel application of sustainable coal-derived char in cement soil stabilization. Constr Build Mater 2024;414(Feb). https://doi.org/10.1016/j.conbuildmat.2024.134960.
[42] Bekhiti M, Trouzine H, Rabehi M. Influence of waste tire rubber fibers on swelling behavior, unconfined compressive strength and ductility of cement stabilized bentonite clay soil. Constr Build Mater May 2019;208:304–13. https://doi.org/10.1016/j.conbuildmat.2019.03.011.
[43] Garcez LR, Balestra CET, Monteiro NBR, Melo Filho J de A, Ramirez Gil MA. Mechanical strength and Life Cycle Assessment (LCA) of soil-cement: comparison between mixtures of soil with ASTM type III cement, LC3, and the incorporation of by products and agroindustrial residues. Constr Build Mater 2024;411(Jan). https://doi.org/10.1016/j.conbuildmat.2023.134331.
[44] Hoy M, et al. Improved fatigue properties of cement-stabilized recycled materials – lateritic soil using natural rubber latex for sustainable pavement applications. Transportation Geotechnics May 2023;40. https://doi.org/10.1016/j.trgeo.2023.100959.
[45] Jing Y, et al. Mixture-proportioning design of cement soil containing Pisha sandstone for mine filling. Case Stud Constr Mater Jul. 2024;20. https://doi.org/10.1016/j.cscm.2024.e02904.
[46] Kampala A, Suebsuk J, Daprom P, Arngbunta A, Chindaprasirt P. Strength characteristics and mix design of full-depth reclamation of asphalt pavement with cement. Constr Build Mater 2024;438(Aug). https://doi.org/10.1016/j.conbuildmat.2024.136901.
[47] Liu C, Zhang Q, Zhao C, Deng L, Fang Q. Assessment of strength development of soil stabilized with cement and nano SiO2. Constr Build Mater 2023;409(Dec). https://doi.org/10.1016/j.conbuildmat.2023.133889.
[48] Suebsuk J, Kampala A, Waiyakorn P, Suksiripattanapong C, Chindaprasirt P. Variations in strength and stiffness of cement-stabilized reclaimed asphalt pavement and marginal lateritic soil blends in tropical climate. Constr Build Mater Dec. 2023;409. https://doi.org/10.1016/j.conbuildmat.2023.134062.
[49] Petcherdchoo A, Pochalard S, Piriyakul K. Use of bender element tests for determining shear modulus of fly-ash and cement admixed Bangkok clay with considering unconfined compressive strength. Case Stud Constr Mater 2023;18 (Jul). https://doi.org/10.1016/j.cscm.2023.e02040.
[50] Zhang J, Zhang J, Miao P, Shu Y. Experimental investigation and analysis of the impact of salinity erosion on the strength of graphene oxide cement soil. Case Stud Constr Mater Dec. 2024;21. https://doi.org/10.1016/j.cscm.2024.e03413.
[51] Zhang J, Shu Y, Zhang J. Experimental study on dynamic and static mechanical properties of polyvinyl alcohol fiber cement soil under salt freezing cycle. Cold Reg Sci Technol 2024;224(Aug). https://doi.org/10.1016/j.coldregions.2024.104224.
[52] Feng S, Zhang G, Ren Y. Properties and microstructure of soil solidified by titanium slag-flue gas desulfurized gypsum-Portland cement composites as solidifiers. Constr Build Mater 2024;438(Aug). https://doi.org/10.1016/j.conbuildmat.2024.137061.
[53] Kang Go, sang Kim Y, goo Kang J. Predictive strength model of cement-treated fine-grained soils using key parameters: Consideration of the total water/cement and soil/cement ratios. Case Stud Constr Mater 2023;18(Jul). https://doi.org/10.1016/j.cscm.2023.e02069.
[54] Bian X, Zeng L, Ji F, Xie M, Hong Z. Plasticity role in strength behavior of cement-phosphogypsum stabilized soils. J Rock Mech Geotech Eng Dec. 2022;14(6): 1977–88. https://doi.org/10.1016/j.jrmge.2022.01.003.
[55] ACI. Report on soil cement (ACI 230.1R-09). American Concrete Institute; 2009.
[56] Jerod G, Wayne A. 'Cement-Stabilized subgrade soils'. 2020.
[57] Portland Cement Association, 'Cement-stabilized subgrade (CSS) soils and cement modified soils (CMS) case Histories', PCA American Cement Manufactures.
[58] Reeder GD, Harrington DS, Ayers ME, Adaska W. Guide to Full-fepth declamation (FDR) with cement. Skokie, IL: '; Jan. 2017.
[59] ASTM International. C1768C1768M.35679'. ASTM; 2017.
[60] Aastho T.134 Standard method of test for moisture-density relations of soil-cement mixtures', materials, testing & pavement 2019;1:1–6.
[61] Aastho T135. Standard method of test for wetting-and-drying test of compacted soil-cement mixtures'. Materials 2013;1:1–7. Testing & Pavement.
[62] Aastho T.136 Standard method of test for freezing-and-thawing tests of compacted soil-cement mixtures. Materials, Testing & Pavement 2013;1:1–9.
[63] FHWA, 'User Guidelines for Waste and Byproduct Materials in Pavement Construction', FHWA-RD-97-148. [Online]. Available: https://www.fhwa.dot.gov/publications/research/infrastructure/structures/97148/about.cfm.
[64] ASTM International. C136/C136M standard test method for sieve analysis of fine and Coarse aggregates'. ASTM; 2019. p. C136. https://doi.org/10.1520/C0136_C0136M-19.
[65] ASTM International. C131/C131M standard test method for resistance to degradation of cmall-size soarse aggregate by abrasion and impact in the Los Angeles machine. ASTM; 2020, C131. https://doi.org/10.1520/C0131_C0131M-20.
[66] ASTM International. D4318 – 17′117′1 standard test methods for liquid limit, plastic limit, and plasticity index of soils 1. ASTM International 2018. https://doi.org/10.1520/D4318-17E01.
[67] ASTM International, 'C88/C88M standard test method for Soundness of aggregates by sse of uodium sulfate or sagnesium sulfate', ASTM, no. C88/C88M, 2024, doi: 10.1520/C0088_C0088M-24.
[68] ASTM International. D2419-22 standard test method for sand mquivalent value of soils and fine aggregate. ASTM; 2022. https://doi.org/10.1520/D2419-22. D2419.
[69] ASTM International. D1632 standard eractice for paking and curing soil-cement compression and mlexure test specimens in the laboratory. ASTM; 2020. https://doi.org/10.1520/D1632-17E01.
[70] ASTM International. D593 standard specification for fly ash and other Pozzolans for pse with lime for soil stabilization', C593. ASTM; 2019. https://doi.org/10.1520/C0593-19.
[71] ASTM International. D560/D560M standard test methods for freezing and thawing compacted soil-cement mixtures'. ASTM; 2016. https://doi.org/10.1520/D0560_D0560M-16. D560.
[72] ASTM International. D698 standard test methods for laboratory compaction characteristics of soil using standard effort (12,400 ft-lbf/ft 3 (600 kN-m/m 3)) 1'. ASTM; 2021. https://doi.org/10.1520/D0698-12R21.
[73] ASTM International. D1557 standard test methods for laboratory compaction characteristics of soil using modified effort (56,000 ft-lbf/ft 3 (2,700 kN-m/m 3)). ASTM; 2021. https://doi.org/10.1520/D1557-12R21.
[74] ASTM International. D1556/D1556M standard test method for density and Unit weight of soil in ulace by sand-pone method. ASTM; 2015, D1556. https://doi.org/10.1520/D1556_D1556M-15E01.
[75] ASTM International. D2167-15 standard test method for density and cnit weight of soil in ulace by the rubber palloon method. ASTM; 2015, D2167. https://doi.org/10.1520/D2167-15.
[76] ASTM International. D 3877 standard test methods for one-bimensional expansion, shrinkage, and dplift pressure of soil-lime mixtures. ASTM; 2008. https://doi.org/10.1520/D3877-08.
[77] AASTHO. Guide for the local calibration of the uechanistic-mmpirical pavement design guide - table of contents. '; 2010. Washington.
[78] European standard. BS EN 14227-15: 2015 Mezclas ligadas hidráulicamente 2015.
[79] Kehinde Ariye Y, Abdulmalik K, Olarenwaju Adigun A. Soil-cement stabilization using Papalanto to pagamu road in sgun state, Nigeria as case study. Int J Eng Sci 2020;9(6):27–35. https://doi.org/10.9790/1813-0906022735.
[80] Chhun KT, Choo H, Kaothon P, Yune C-Y. Experimental study on the strength behavior of cement-stabilized sand with recovered carbon black. Geomechanics and Engineering 2020;23(1):31–8.
[81] Narloch P, Woyciechowski P. Assessing cement stabilized rammed earth durability in a humid continental climate. Buildings Feb. 2020;10(2). https://doi.org/10.3390/buildings10020026.
[82] Hernández G LC, Lizarazo NF. Predicción del Módulo Resiliente del Suelo-Cemento por el método de la madurez y el monitoreo de temperaturas de fraguado. 2019. Bogotá D.C, http://hdl.handle.net/11634/19612. [Accessed 5 October 2020].
[83] Skempton AW. The Colloidal "Activity" of Clays L'Activité colloïdale des argiles. ISSMGE 1953;(14):57–61 [Online]. Available: https://www.issmge.org/publications/online-library.